Electronic Supplementary Material (ESI) for Journal of Materials Chemistry A.

Electronic Supplementary Information (ESI)

Controllable Sulfuration Engineered NiO Nanosheets with Enhanced Capacitance for High Rate Supercapacitors

Shude Liu [a], Su Chan Lee [a,b], Umakant M Patil [a], Chaiti Ray [a], K. Vijaya Sankar [a], Kan Zhang [c], Aniruddha Kundu [a], Shinill kang [a], Jong Hyeok Park [c] and Seong Chan Jun*[a]

[a]School of Mechanical Engineering, Yonsei University, 50 Yonsei-ro, Seodaemun-gu, Seoul 120-749, South Korea.

[b]Center for Energy Convergence Research, Korea Institute of Science and Technology, Hwarang-ro 14-gil 5, Seongbuk-gu, Seoul 136-791, South Korea.

[c]Department of Chemical and Biomolecular Engineering, Yonsei University, 50 Yonsei-ro, Seodaemun-gu, Seoul 120-749, South Korea.

**Corresponding author:*

E-mail: scj@yonsei.ac.kr

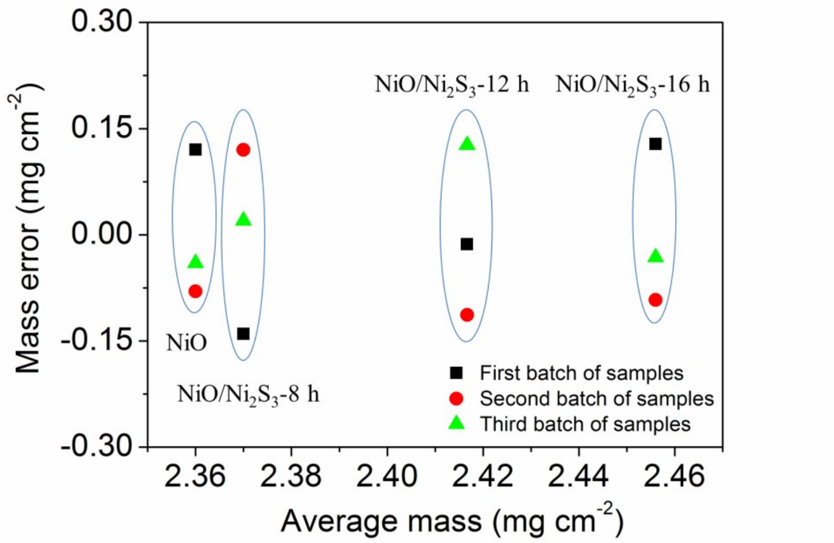

Figure S1 The average mass loading as functions of mass error for the as-synthesized samples in three independent experiments.

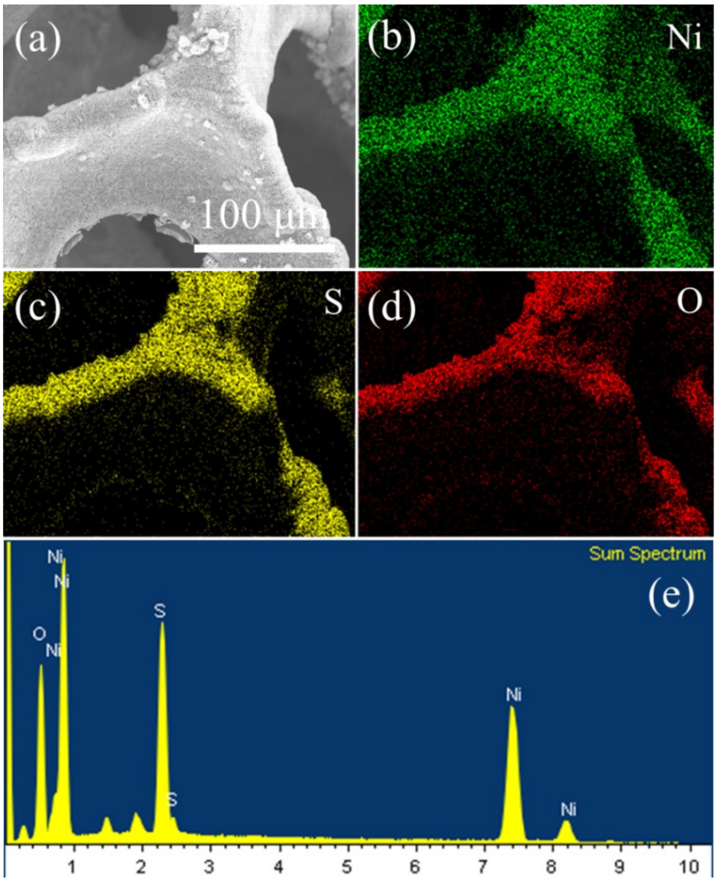

Figure S2 (a) SEM image and the corresponding elemental mapping images of Ni (b), S (c), and O (d), and EDS spectrum (e) of the NiO/Ni_3S_2-12 h.

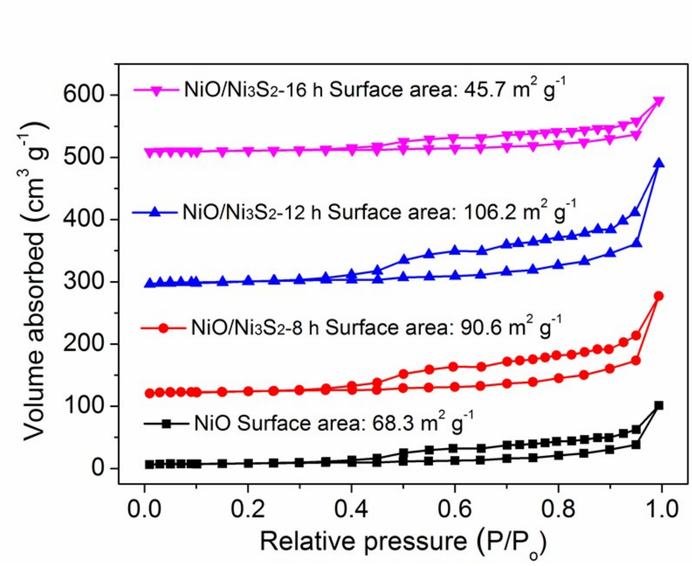

Figure S3 Brunauer−Emmett−Teller (BET) specific surface areas of as-synthesized samples.

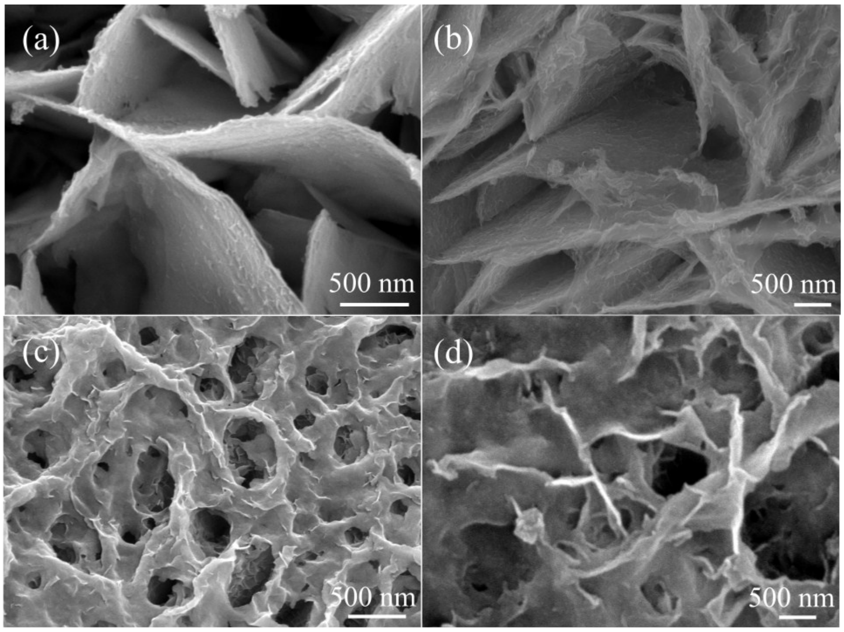

Figure S4 Typical SEM images of NiO/Ni_3S_2-12 h formed at: (a) 70 °C, (b) 100 °C, (c) 140 °C and (d) 180 °C.

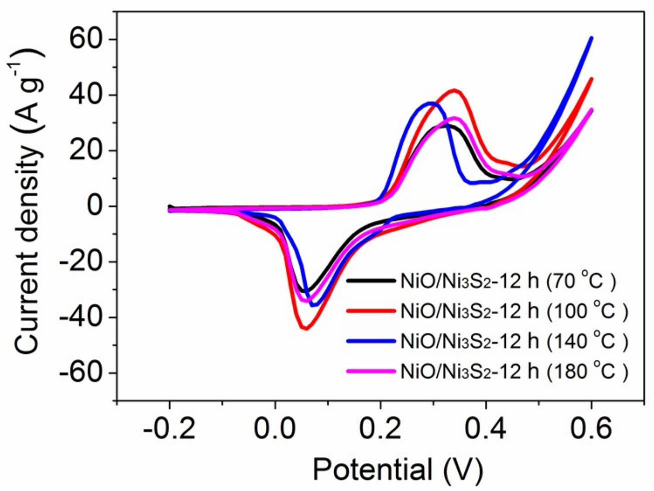

Figure S5 Comparison of the CV plots for NiO/Ni_3S_2-12 h (T = 70 °C, 100 °C, 140 °C and 180 °C) measured at a scan rate of 5 mV s^{-1}.

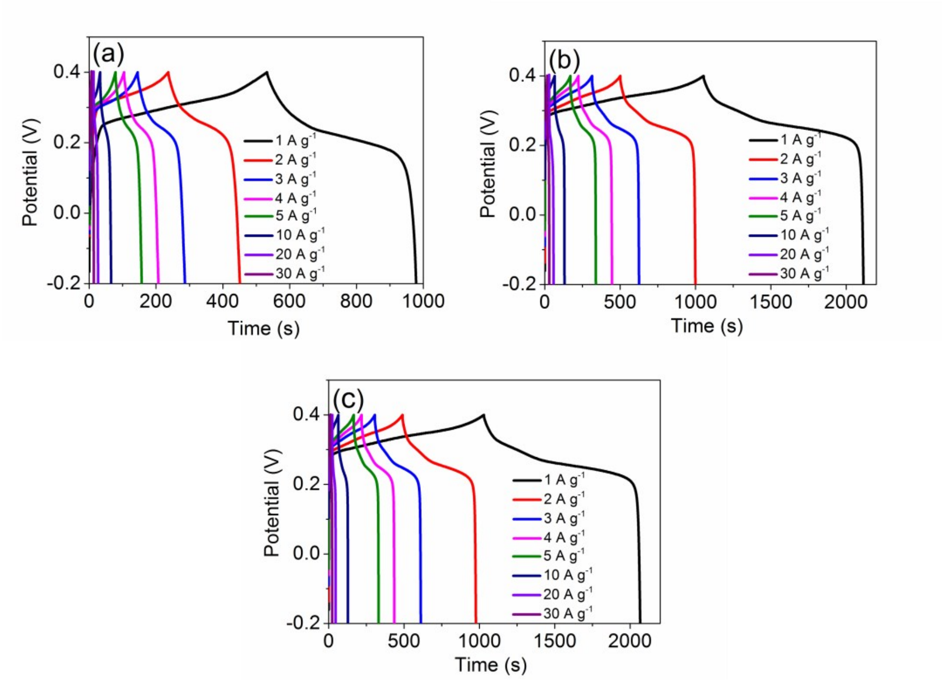

Figure S6 Galvanostatic charge–discharge curves of (a) NiO, (b) NiO/Ni_3S_2-8 h, and (c) NiO/Ni_3S_2-16 h electrodes measured at different current densities.

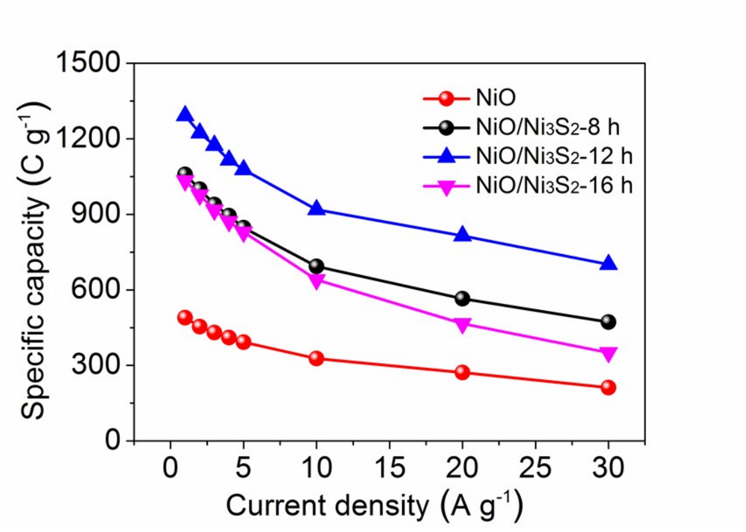

Figure S7 The specific capacities of the as-synthesized samples at different current densities.

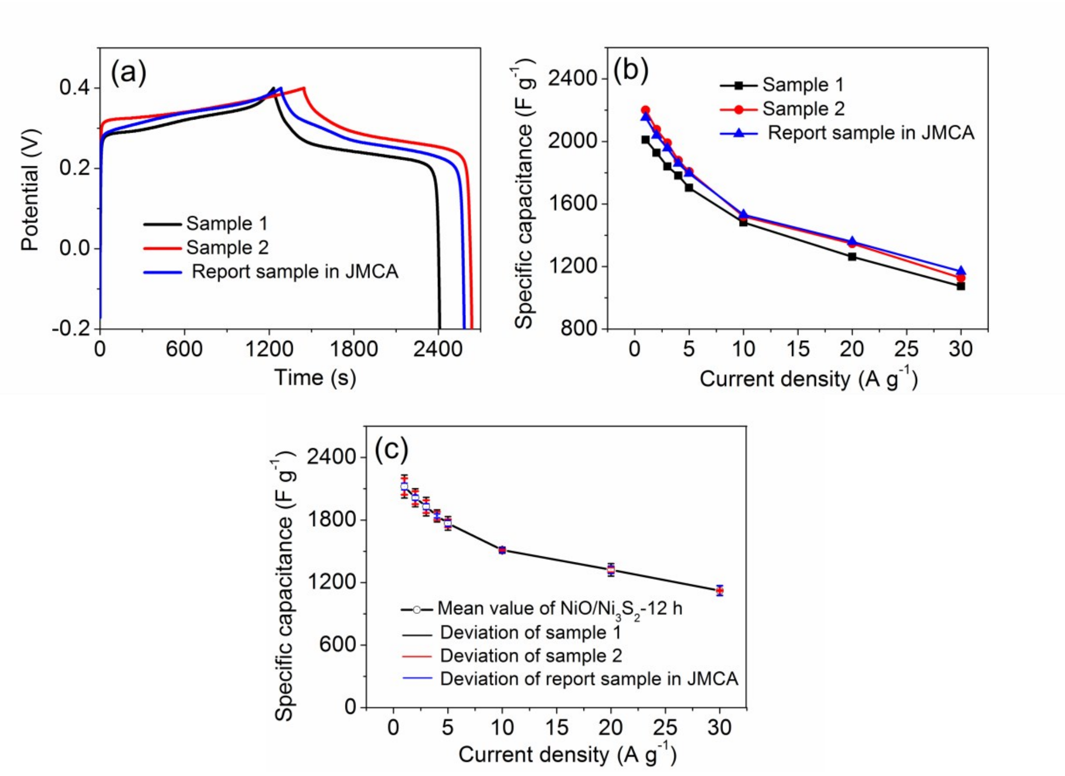

Figure S8 (a) GCD curves of three batches NiO/Ni_3S_2-12 h at current density of 1 A g^{-1}. (b) Specific capacitances as a function of discharge current densities. (c) Representing average value of the specific capacitances for the three batches NiO/Ni_3S_2-12 h.

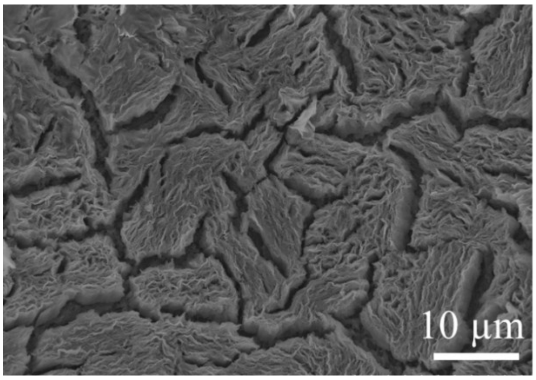

Figure S9 SEM image of the NiO/Ni_3S_2-12 h electrode after 5 000 cycling test.

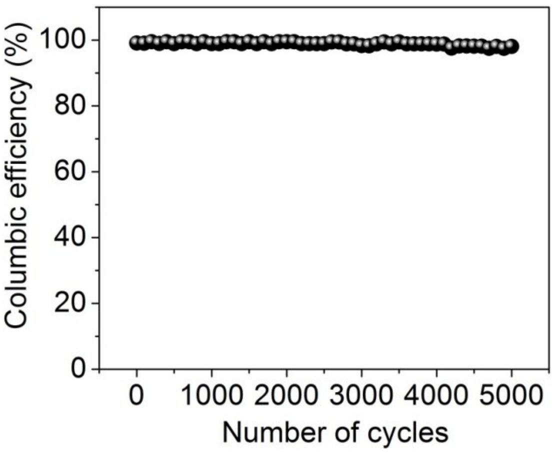

Figure S10 Coulombic efficiency of NiO/Ni_3S_2-12 h electrode during 5 000 successive charge/discharge process.

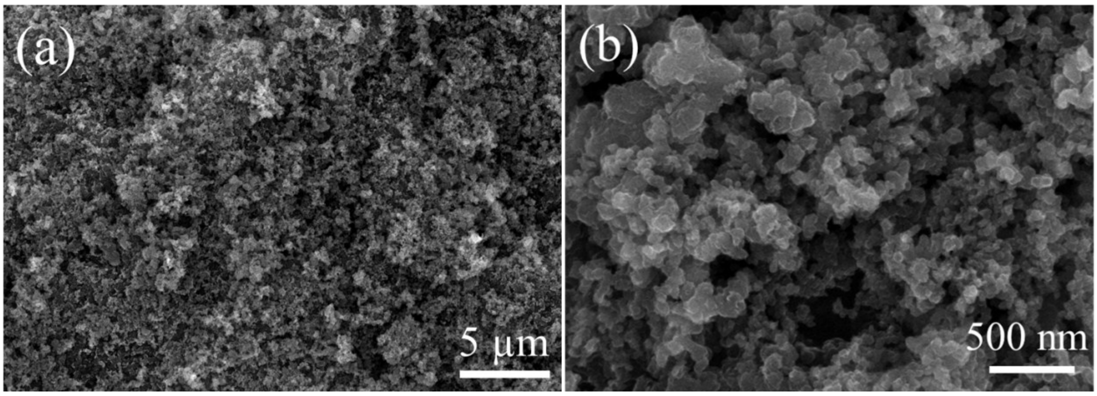

Figure S11 SEM images of activated carbon.

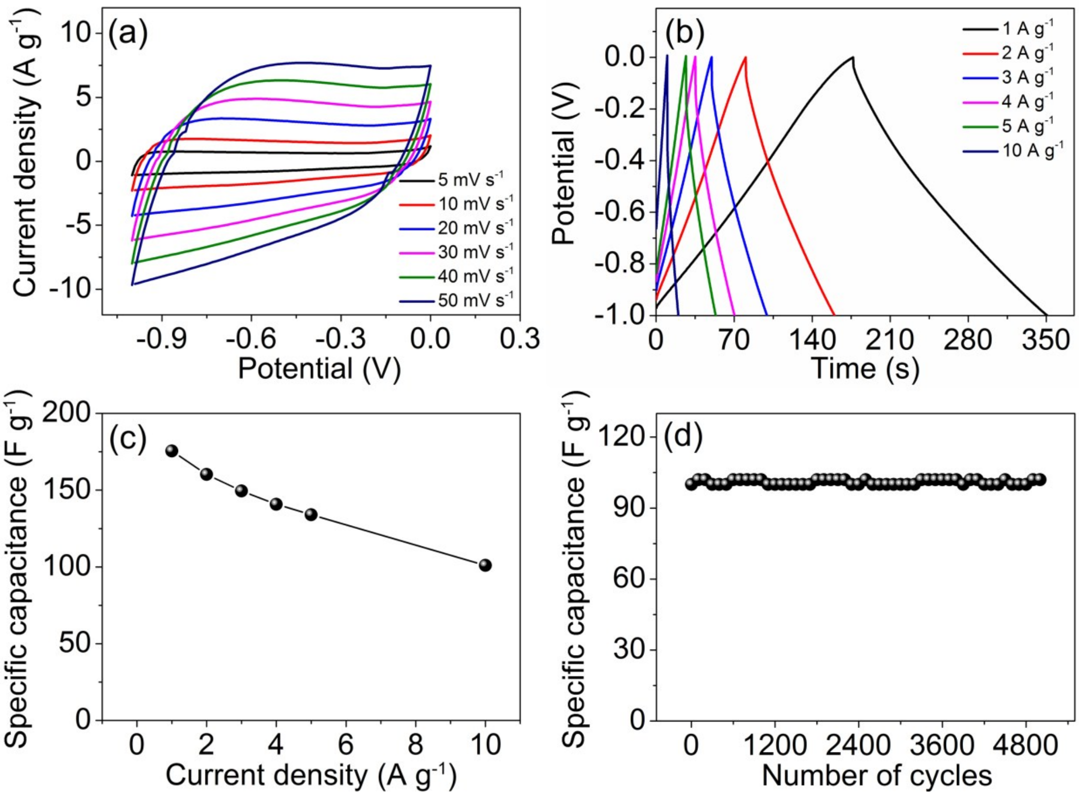

Figure S12 (a) CV curves measured at various scan rates, (b) GCD curves recorded at different current densities, (c) specific capacitance versus discharge current density, and (d) cycling stability of the AC electrode measured in a 3 M KOH electrolyte.

The CV curve of the AC electrode (Figure S12a) exhibits typical rectangular shapes without obvious distortion, which implies a good capacitance feature and fast diffusion of the electrolyte ions. GCD curves of the AC electrode (Figure S12b) are linear and exhibit near mirror-image responses at different current densities from 1 to 10 A g^{-1}, which further confirms that the material possesses an ideal capacitor behavior. The specific capacitance of the AC electrode calculated from the GCD curves is shown in Figure S12c. Specifically, the AC electrode shows specific capacitance values of 176, 160, 149, 141, and 134 F g^{-1} at 1, 2, 3, 4, and 5 A g^{-1}, respectively. Even at a relatively high current density of 10 A g^{-1}, the specific capacitance remains at 101 F g^{-1}, which indicates that the AC electrode delivers a high rate capability. Moreover, the AC electrode exhibits a great electrochemical stability with 102% capacitance retention over 5 000 cycles (Figure S12d).

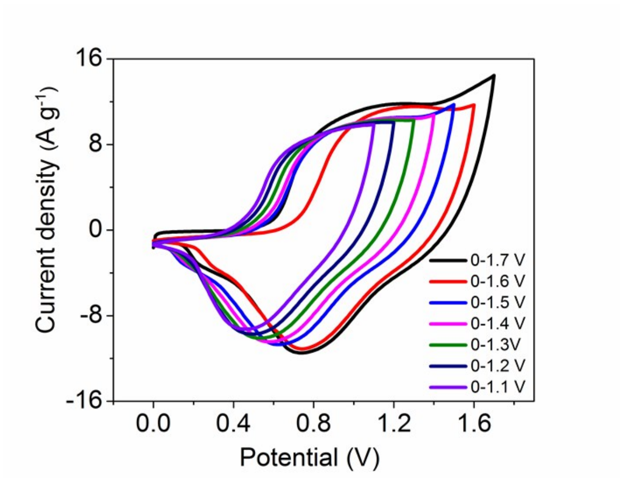

Figure S13 CV curves of the NiO/Ni_3S_2//AC ASC device under different potential windows at a scan rate of 50 mV s^{-1}.

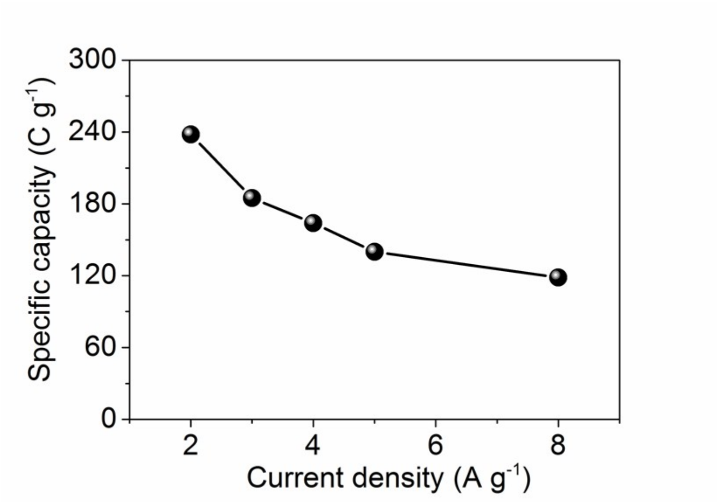

Figure S14 The specific capacity of the assembled NiO/Ni_3S_2-12 h//AC ASC device at different current densities.

Table S1 Electrochemical performances comparison of the NiO/Ni_3S_2 hetero-nanosheets with previous reports on nickel-based electrode materials.

Materials	Specific capacitance (current destiny/scan rate)	Rate capability	Ref.
NiO nanoslices	116 $F\ g^{-1}$ at 0.5 $A\ g^{-1}$; 52 $F\ g^{-1}$ at 5 $A\ g^{-1}$	44.8%	S1
NiO nanoparticles	260 $F\ g^{-1}$ at 0.5 $A\ g^{-1}$; 89 $F\ g^{-1}$ at 5 $A\ g^{-1}$	34.2%	S1
NiO nanoparticles/CNT	1088.44 $F\ g^{-1}$ at 5 $mV\ s^{-1}$; 261.59 $F\ g^{-1}$ at 50 $mV\ s^{-}$	33%	S2
$NiO@MnO_2$ core–shell nanocomposites	266.7 $F\ g^{-1}$ at 0.5 $A\ g^{-1}$; 147.3 $F\ g^{-1}$ at 10 $A\ g^{-1}$	55.2%	S3
CNT@NiO nanosheets	996 $F\ g^{-1}$ at 1 $A\ g^{-1}$; 500 $F\ g^{-1}$ at 20 $A\ g^{-1}$	50.2%	S4
$Co_3O_4@NiO$ hierarchical nanowire arrays	1236.67 $F\ g^{-1}$ at 1 $A\ g^{-1}$; 836.7 $F\ g^{-1}$ at 20 $A\ g^{-1}$	66.7%	S5
$Ni(OH)_2@Mn_2O_3$ particles	2109.5 $F\ g^{-1}$ at 0.5 $A\ g^{-1}$; 718.2 $F\ g^{-1}$ at 6 $A\ g^{-1}$	34%	S6
NiAl-layered double hydroxide (LDH) nanosheets/hollow carbon nanofibers	1613 $F\ g^{-1}$ at 1 $A\ g^{-1}$; 1110 $F\ g^{-1}$ at 10 $A\ g^{-1}$	68.8%	S7
Graphene sheets/NiCo-LDH nanoflakes	1980.7 $F\ g^{-1}$ at 1 $A\ g^{-1}$; 1274.7 $F\ g^{-1}$ at 15 $A\ g^{-1}$	64.4%	S8
$MnCo_2O_4@Ni(OH)_2$ nanoflowers	2154 $F\ g^{-1}$ at 5 $A\ g^{-1}$; 702 $F\ g^{-1}$ at 20 $A\ g^{-1}$	32.6 %	S9
NiMn-LDH nanosheets /GO	2246.63 $F\ g^{-1}$ at 1 $A\ g^{-1}$; 1333.33 $F\ g^{-1}$ at 20 $A\ g^{-1}$	59.35%	S10
NiCo-LDHs/nitrogen-doped carbonized bacterial cellulose	1949.5 $F\ g^{-1}$ at 1 $A\ g^{-1}$; 1066 $F\ g^{-1}$ at 10 $A\ g^{-1}$	54.7%	S11
NiCo-LDHs particles/RGO	2130 $F\ g^{-1}$ at 1 $A\ g^{-1}$; 1235 $F\ g^{-1}$ at 10 $A\ g^{-1}$	58%	S12
Ni_3S_2 hollow structure@β-NiS nanorods	1158 $F\ g^{-1}$ at 2 $A\ g^{-1}$; 670 $F\ g^{-1}$ at 50 $A\ g^{-1}$	57.6%	S13
NiO/Ni_3S_2 hetero-nanosheets	2153 $F\ g^{-1}$ at 1 $A\ g^{-1}$; 1359 $F\ g^{-1}$ at 20 $A\ g^{-1}$	63.1%	Present work

Table S2 Comparison of energy and power densities of the reported nickel based oxides and sulfides for ASC devices and the present work

ASC devices	Energy density (Wh kg^{-1}) and the corresponding power density (W kg^{-1})	Ref.
Ni_3S_2/CNT//AC	19.8 Wh kg^{-1} at 798 W kg^{-1}	S14
NiS_2//rGO	32.76 Wh kg^{-1} at 954 W kg^{-1}	S15
$NiCo_2S_4$//AC	25.5 Wh kg^{-1} at 334 W kg^{-1}	S16
$CoNi_2S_4$//AC	33.9 Wh kg^{-1} at 409 W kg^{-1}	S17
Ni_3S_2/carbon fiber//carbon fiber	25.8 Wh kg^{-1} at 425 W kg^{-1}	S18
NiO/Ni_3S_2//AC	52.9 W h kg^{-1} at 1600 W kg^{-1}	Present work

S1. S.-I. Kim, J.-S. Lee, H.-J. Ahn, H.-K. Song and J.-H. Jang, *ACS applied materials & interfaces*, 2013, **5**, 1596-1603.
S2. J. Cheng, B. Zhao, W. Zhang, F. Shi, G. Zheng, D. Zhang and J. Yang, *Advanced Functional Materials*, 2015, **25**, 7381-7391.
S3. J. Chen, Y. Huang, C. Li, X. Chen and X. Zhang, *Applied Surface Science*, 2016, **360**, 534-539.
S4. H. Yi, H. Wang, Y. Jing, T. Peng and X. Wang, *Journal of Power Sources*, 2015, **285**, 281-290.
S5. Q. Hu, Z. Gu, X. Zheng and X. Zhang, *Chemical Engineering Journal*, 2016, **304**, 223-231.
S6. Q. Ren, R. Wang, H. Wang, J. Key, D. J. Brett, S. Ji, S. Yin and P. K. Shen, *Journal of Materials Chemistry A*, 2016, **4**, 7591-7595.
S7. F. He, Z. Hu, K. Liu, S. Zhang, H. Liu and S. Sang, *Journal of Power Sources*, 2014, **267**, 188-196.
S8. T. Yan, R. Li and Z. Li, *Materials Research Bulletin*, 2014, **51**, 97-104.
S9. Y. Zhao, L. Hu, S. Zhao and L. Wu, *Advanced Functional Materials*, 2016, **26**, 4085-4093.
S10. J. Chen, X. Wang, J. Wang and P. S. Lee, *Advanced Energy Materials*, 2015, **6**, 1-8.
S11. F. Lai, Y. E. Miao, L. Zuo, H. Lu, Y. Huang and T. Liu, *Small*, 2016, **12**, 3235-3244.
S12. M. Jana, S. Saha, P. Samanta, N. C. Murmu, N. H. Kim, T. Kuila and J. H. Lee, *Journal of Materials Chemistry A*, 2016, **4**, 2188-2197.
S13. W. Li, S. Wang, L. Xin, M. Wu and X. Lou, *Journal of Materials Chemistry A*, 2016, **4**, 7700-7709
S14. C.-S. Dai, P.-Y. Chien, J.-Y. Lin, S.-W. Chou, W.-K. Wu, P.-H. Li, K.-Y. Wu and T.-W. Lin, *ACS applied materials & interfaces*, 2013, **5**, 12168-12174.
S15. Y. Ruan, J. Jiang, H. Wan, X. Ji, L. Miao, L. Peng, B. Zhang, L. Lv and J. Liu, *Journal of Power Sources*, 2016, **301**, 122-130.
S16. H. Chen, J. Jiang, L. Zhang, D. Xia, Y. Zhao, D. Guo, T. Qi and H. Wan, *Journal of Power Sources*, 2014, **254**, 249-257.
S17. W. Hu, R. Chen, W. Xie, L. Zou, N. Qin and D. Bao, *ACS applied materials & interfaces*, 2014, **6**, 19318-19326.
S18. W. Yu, W. Lin, X. Shao, Z. Hu, R. Li and D. Yuan, *Journal of Power Sources*, 2014, **272**, 137-143.